Ezh2 controls B cell development through histone H3 methylation and *Igh* rearrangement

I-hsin Su[1], Ashwin Basavaraj[1], Andrew N. Krutchinsky[2], Oliver Hobert[3], Axel Ullrich[4], Brian T. Chait[2] and Alexander Tarakhovsky[1]

Published online 23 December 2002; doi:10.1038/ni876

Polycomb group protein Ezh2 is an essential epigenetic regulator of embryonic development in mice, but its role in the adult organism is unknown. High expression of Ezh2 in developing murine lymphocytes suggests Ezh2 involvement in lymphopoiesis. Using Cre-mediated conditional mutagenesis, we demonstrated a critical role for Ezh2 in early B cell development and rearrangement of the immunoglobulin heavy chain gene (*Igh*). We also revealed Ezh2 as a key regulator of histone H3 methylation in early B cell progenitors. Our data suggest Ezh2-dependent histone H3 methylation as a novel regulatory mechanism controlling *Igh* rearrangement during early murine B cell development.

Commitment of cells to a particular lineage and their maintenance in a differentiated state involves the activation of limited gene sets while leaving the rest of the genome in a repressed state[1]. The cell type–specific gene expression pattern is stabilized by changes in the chromatin structure associated with active and silent genomic loci[2]. These heritable chromatin modifications can be maintained by counteraction of transcriptional activators of the trithorax group (TrxG) proteins and repressors of the polycomb group (PcG) proteins[2].

The PcG proteins are organized in two to five megadalton (MD) complexes that exert their influence on gene expression through local chromatin modifications[3]. At least two distinct mechanisms of gene repression are utilized by PcG proteins. The PcG complex that contains the EED, EZH2 and EZH1 proteins can control gene repression through the recruitment of a histone deacetylase followed by local chromatin deacetylation[4,5]. The other PcG complex—polycomb repressive complex 1 (PRC-1)—contains polycomb 2 (HPC2), polyhomeotic (HPH), BMI1 and Ring-finger protein 1 (RING1) proteins that negatively regulate chromatin accessibility promoted by the chromatin remodeling SWI-SNF complex[6].

The physiological significance of PcG protein–mediated gene regulation is underscored by developmental abnormalities found in mice deficient in the PcG proteins. Targeted disruption of the gene encoding PcG protein results in ectopic expression of Hox transcription factors, which control cell type–specific gene expression[7]. As a consequence, mice deficient for distinct PcG proteins develop skeletal transformations[8], show male-to-female sex reversal[9] or neurological abnormalities[8].

A common consequence of PcG deficiencies is the defective development and activation of lymphocytes. For example, inactivation of mammalian homologs of the *Drosophila* gene *posterior sex combs* (*Psc*), *Bmi1* or *mel-18* (also termed *Zfp144*), causes a severe block in B cell development that leads to B cell lymphopenia in the mutant mice[8,10]. Similar to *Bmi1* and *mel-18*, the presence of *rae28*, a mammalian ortholog of the *Drosophila* gene *polyhomeotic* (*Ph*), is required for normal B cell development, as shown by reduced generation of pre-B and immature B cells from *rae28*-deficient fetal liver hematopoietic progenitors[11]. Deficiency in *Cbx2* (also termed *M33*), the murine counterpart of the *Drosophila* gene *polycomb* (*Pc*), does not affect lymphocyte development but renders splenic B cells unresponsive to lipopolysaccharide (LPS)[12].

Several lines of evidence support the involvement of the PcG protein Ezh2—a mammalian homolog of the *Drosophila* PcG protein E(Z) (originally termed Enx-1)[13,14]—in chromatin remodeling, as well as in lymphocyte development and activation. *Ezh2* is distinct among the PcG family of genes because it contains the evolutionarily conserved SET domain that is responsible for histone H3 methyltransferase activity (HMTase) of E(Z). The E(Z) methylates *in vitro* lysine 9 (H3-K9) and lysine 27 (H3-K27) of histone H3[15–17]. In general, methylation of lysines within the histone H3 N-terminal tail causes stable changes in chromatin that define the activation status of the gene. Thus, the methylation of H3-K9 or H3-K4 by distinct HMTases is associated with stable gene repression or transcriptional activation, respectively[18]. However, neither the ability of mouse Ezh2 to control histone H3 methylation *in vitro* and *in vivo* nor the physiological significance of Ezh2-mediated H3 lysine methylation are known.

In mice, Ezh2 is most abundant at sites of embryonic lymphopoiesis, such as fetal liver and thymus[14]. Up-regulation of Ezh2 in proliferating human germinal center B cells (centroblasts)[19] and mitogen-stimulated lymphocytes[20] suggests an important role for this protein in B cell division. The potential importance of Ezh2 in lymphocyte activation is further supported by its association with Vav, one of the key regulators of the receptor-mediated signaling in lymphocytes[13].

Functional analysis of Ezh2 in lymphocyte development is complicated by the early embryonic death of Ezh2-deficient mice[21]. To circumvent the lethal effect of the *Ezh2* null mutation, we employed the Cre-*loxP* technology for conditional gene inactivation[22]. Here we demonstrate that Ezh2

[1]Laboratory of Lymphocyte Signaling and [2]Laboratory of Mass Spectrometry and Gaseous Ion Chemistry, The Rockefeller University, New York, NY 10021 USA. [3]Department of Biochemistry and Molecular Biophysics, Center for Neurobiology and Behavior, Columbia University, College of Physicians and Surgeons, New York, NY 10032, USA. [4]Max Planck Institute for Biochemistry, Department of Molecular Biology, D-82152 Martinsried, Germany. Correspondence should be addressed to A.T. (tarakho@mail.rockefeller.edu).

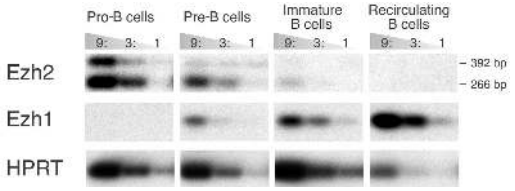

Figure 1. Expression of Ezh2 and Ezh1 mRNA in B lineage cells. Total RNA isolated from FACS-purified B cell subpopulations was reverse-transcribed with oligo(dT) primers and threefold serial dilutions of cDNA were used for PCR amplification. The PCR products were visualized by Southern blotting with Ezh2- or Ezh1-specific probes. The two Ezh2-specific PCR products reflect alternative splicing of the Ezh2 mRNA. RT-PCR analysis of HPRT mRNA expression was used as a cDNA loading control.

controls B cell development through the regulation of histone H3 methylation and immunoglobulin heavy chain gene (*Igh*) rearrangement. We suggest that Ezh2-dependent histone H3 methylation leads to chromatin modification required for normal *Igh* rearrangement, which is critical for early B cell development.

Results

Ezh2 expression in B lineage cells

Analysis of Ezh2 mRNA expression in B lineage cells isolated from wild-type 129Sv mice showed a reverse correlation between Ezh2 expression and the degree of B cell differentiation and maturation (**Fig. 1**). In B cell progenitors, Ezh2 expression was highest in pro-B cells ($IgM^-B220^+CD43^+$) and was much lower in pre-B cells ($IgM^-B220^+CD43^-$). Further differentiation of B cells led to a reduction in Ezh2 expression in immature B cells ($B220^{int}IgM^+gD^-$) and, most profoundly, in mature recirculating ($B220^{hi}IgM^+IgD^+$) B cells. In contrast to Ezh2, the expression levels of Ezh1, which harbors a SET domain and shows 67% amino acid identity to Ezh2[23], was low in pro-B and pre-B cells but increased in immature and recirculating B cells. The high abundance of Ezh2 mRNA in early B cell progenitors points to a possible involvement of Ezh2 in the regulation of early B cell development in the bone marrow, whereas Ezh1 may play a role in the peripheral B cells.

Conditional inactivation of *Ezh2*

Using a gene targeting approach, we generated embryonic stem (ES) cells and mice in which exons encoding the SET domain of *Ezh2* are flanked with *loxP* sequences, which can be recognized by Cre recombinase (**Fig. 2a,b**). The SET domain was originally described as a sequence homolog to the three *Drosophila* genes *suppressor of variegation (3–9)* (*Su(var)3-9*), *enhancer of zeste* (*E(Z)*) and trithorax (*trx*)[24]. The SET domain was chosen as a target for *Ezh2* inactivation because this domain is essential for functioning of the *Drosophila* homolog of *Ezh2*, *E(Z)*[25].

Insertion of the two *loxP* sequences into the *Ezh2* genomic locus did not alter Ezh2 expression, and mice homozygous for the *loxP*-flanked *Ezh2* allele ($Ezh2^{fl/fl}$) were viable and developed normally. By crossing $Ezh2^{fl/fl}$ mice with transgenic mice that expressed Cre recombinase in the germ line, we generated mice heterozygous for the modified *Ezh2* allele ($Ezh2^{-/+}$). Whereas $Ezh2^{-/+}$ mice developed and lived normally, crossing of $Ezh2^{-/+}$ mice never yielded any $Ezh2^{-/-}$ pups. We took the fact that the deletion of exons encoding the SET domain in *Ezh2* led to embryonic lethality as proof of the reliability of the chosen strategy of *Ezh2* inactivation, as complete deletion of Ezh2 in the germ line also resulted in early death of the mutant embryos[21].

To achieve the inducible inactivation of Ezh2, $Ezh2^{fl/+}$ mice were bred to Mx-Cre transgenic mice harboring the Cre-recombinase transgene driven by the interferon-inducible Mx promoter[26]. The deletion of Ezh2 was induced by repetitive intraperitoneal (i.p.) injections of poly(I)•poly(C)[26]. Unless specified, mice received three poly(I)•poly(C) injections at 2-day intervals and were sacrificed on day 10 following the last injection. Southern blot analysis of the DNA derived from various lymphoid organs of the poly(I)•poly(C)-injected Mx-Cre $Ezh2^{fl/fl}$ mice revealed virtually

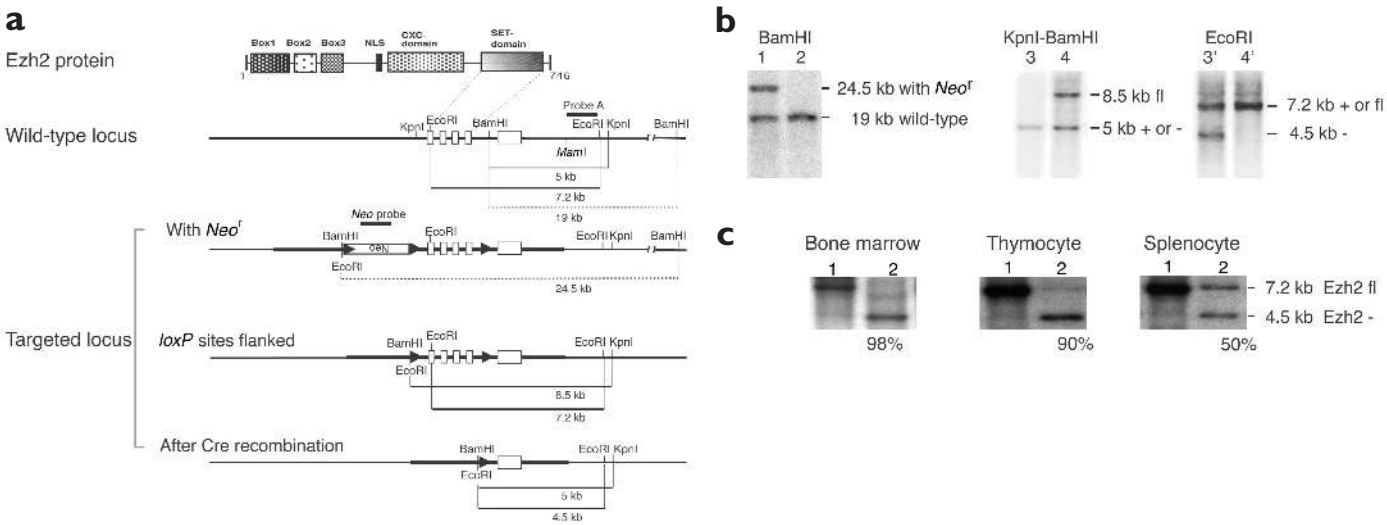

Figure 2. Conditional inactivation of *Ezh2*. (**a**) The domain structure of Ezh2 protein, part of the *Ezh2* genomic locus and the *Ezh2*-targeted locus before and after Cre-mediated recombination are shown. The small open boxes indicate exons encoding the SET domain. The large open box corresponds to the last exon of *Ezh2* encoding the 3′ untranslated region. The arrows correspond to the *loxP* sequences. neo^r, neomycin phosphotransferase gene. The sizes of the expected restriction enzyme–digested DNA fragments that were recognized by probe A (the 1-kb *Eco*RI-*Mam*I fragment) are shown. (**b**) Genomic DNA isolated from ES cells was digested with *Bam*HI and analyzed by Southern blotting. Probe A recognizes a 19-kb fragment derived from the wild-type allele (lanes 1 and 2) and a 24.5-kb fragment from the neo^r-containing targeted allele (lane 1). DNA isolated from the pIC-Cre transiently transfected ES clones was digested with *Kpn*I-*Bam*HI. Loss of neo^r only or together with the *loxP*-flanked exons gave rise to 8.5-kb (lane 4) and 5-kb (lanes 3 and 4) DNA fragments, respectively. To distinguish between the wild-type or Cre-mediated deleted *Ezh2* alleles, DNA was digested with *Eco*RI. The 4.5-kb and 7.2-kb DNA fragments correspond to the deleted (lane 3′) or *loxP*-flanked (lanes 3′ and 4′) alleles, respectively. (**c**) $Ezh2^{fl/f}$ (lane 1) and $Ezh2^{fl/fl}$ Mx-Cre (lane 2) mice were injected with poly(I)•poly(C). The efficiency of the *Cre*-mediated Ezh2 deletion was quantified by densitometry analysis of Southern blots hybridized with probe A. The *loxP*-flanked (Ezh2 fl) and deleted (Ezh2 –) *Ezh2* alleles gave rise to 7.2-kb and 4.5 kb DNA fragments, respectively. The percentage values indicate the deletion efficiency.

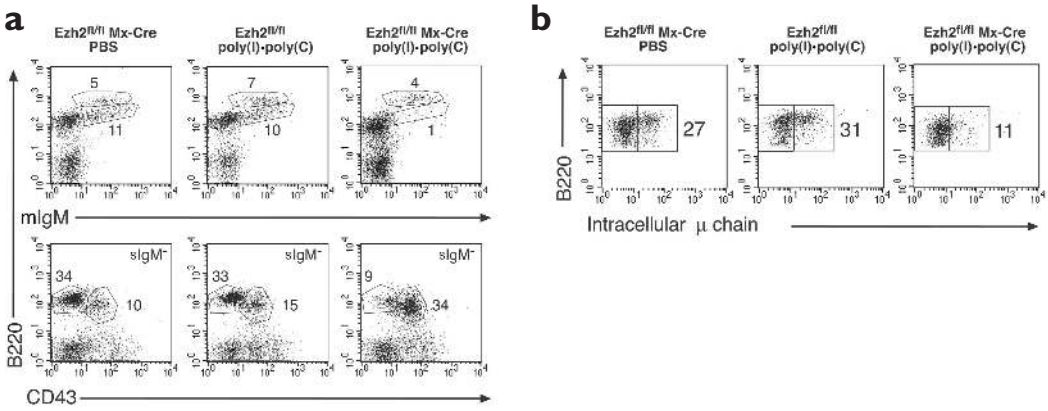

Figure 3. Impaired development of Ezh2-deficient B cells. (**a**) Bone marrow cells were isolated from the control and experimental mice on day 10 after the last PBS or poly(I)•poly(C) injection. Expression of the indicated surface proteins was analyzed by FACS. The lower panel shows the expression of CD43 and B220 within the subpopulation of surface IgM–negative (sIgM$^-$) bone marrow cells. (**b**) The expression of intracellular μ chain in B220$^+$CD43$^+$ pro-B cells was analyzed by FACS. The numbers indicate the percentages of gated cells. The FACS data are representative of ten independent experiments.

complete inactivation of Ezh2 in the bone marrow (98%) and thymus (95%); however, in the spleen, deletion occurred with 50% efficiency (**Fig. 2c**). Although cells homozygous for the *Ezh2* deletion contained mRNA corresponding to the Cre-modified *Ezh2* gene (*Ezh2*$^{-/-}$), SET domain–deficient truncated Ezh2 protein could not be detected (data not shown). These data indicated that deletion of exons encoding the SET domain leads to complete *Ezh2* inactivation.

Impaired development of Ezh2-deficient B cells

The frequencies and absolute numbers of cells comprising various lymphocyte subpopulations were similar in the bone marrow and peripheral lymphoid organs of the poly(I)•poly(C)-injected Ezh2$^{fl/fl}$ and PBS-injected Mx-Cre Ezh2$^{fl/fl}$ mice analyzed on day 10 following the last injection (**Fig. 3a**). This result excluded the toxicity of poly(I)•poly(C) as a possible cause of changes in B cell development. Analysis of Ezh2-deficient bone marrow cells derived from the poly(I)•poly(C)-injected Mx-Cre Ezh2$^{fl/fl}$ mice showed unaltered development of pro-B cells (IgM$^-$B220$^+$CD43$^+$) followed by a decrease in the frequencies and numbers of pre-B (IgM$^-$B220$^+$CD43$^-$) and immature B cells (IgM$^+$B220^{int}). Complete deletion of Ezh2 in pro-B cells was confirmed by Southern blot, polymerase chain reaction (PCR) and reverse-transcribed PCR (RT-PCR) analysis (**Supplementary Fig. 1** online). Collectively, the observed alteration in development of Ezh2-deficient B cells revealed Ezh2 as a component of the checkpoint mechanism that controls the pro-B to pre-B cell transition.

Deletion of Ezh2 at nearly 100% efficiency in the bone marrow of the poly(I)•poly(C)-injected Mx-Cre Ezh2$^{fl/fl}$ mice probably also led to Ezh2-deficiency in stromal cells that support B cell development *via* the secretion of various cytokines[27]. Hence, observed changes in the development of Ezh2-deficient B cells may not have been cell-autonomous. To address this question, bone marrow transfer experiments were performed. To distinguish the donor bone marrow–derived cells from the recipient cells, surface expression of Ly9.1 was used as a marker for the donor-derived cells. Ly9.1$^+$ Ezh2-deficient bone marrow cells were isolated from poly(I)•poly(C)-treated Mx-Cre Ezh2$^{fl/fl}$ mice and transferred either alone or in combination with the wild-type bone marrow cells into lethally irradiated Ly9.1-negative C57BL/6 mice. The resulting bone marrow chimeras were analyzed at different time points after transplantation. The analysis of the bone marrow chimeras 28 days after transplantation revealed a block in pro-B to pre-B cell development, similar to that observed in the bone marrow of poly(I)•poly(C)-injected Mx-Cre Ezh2$^{fl/fl}$ mice (**Supplementary Fig. 2** online). Cotransfer of the wild-type and Ezh2$^{-/-}$ bone marrow cells did not revert the block in Ezh2$^{-/-}$ B cell development and the block was so profound that even twenty weeks after transplantation, the number of Ezh2$^{-/-}$ IgM$^+$ B cells was below 1% of the control values (data not shown). These data prove the cell-autonomous nature of defective Ezh2-deficient B cell development.

Reduced μ chain expression in Ezh2-deficient cells

The pro-B to pre-B cell differentiation and expansion of pre-B cells are governed by signals derived from the surface expressed pre-B cell receptor (pre-BCR)[28]. Thus defects either in pre-BCR formation or impairment of its signaling properties may severely impair the pro-B to pre-B cell development. About 25–30% of the pro-B cells derived from control mice expressed the intracellular μ chain, as determined by intracellular staining with the μ chain–specific antibody M41. In contrast to the control pro-B cells, the Ezh2-deficient pro-B cells did not form a well-defined population of B220^{int}, intracellular μ$^+$ cells and the overall frequency of B220$^+$, intracellular μ$^+$ cells was reduced to 30% (**Fig. 3b**). The reduction in frequencies of μ chain expressing cells correlates directly with a three-fold reduction in μ chain mRNA expression in Ezh2$^{-/-}$ pro-B cells compared to control pro-B cells. In contrast, Ezh2-deficiency did not affect the frequency of pro-B cells expressing intracellular κ light chain (**Supplementary Fig. 3** online). The latter result therefore suggests Ezh2 specifically affects μ chain production.

Igh transgene rescues Ezh2-deficient B cell development

If the defective heavy chain rearrangement is the main cause of impaired Ezh2-deficient B cell development, the expression of a prerearranged heavy chain should rescue Ezh2-deficient pro-B cells. To test such a possibility, Mx-Cre Ezh2$^{fl/fl}$ mice were bred with mice carrying rearranged V_HD-$_HJ_H$ (B1-8) inserted at the J_H locus (B1-8i) by homologous recombination[29]. The Ezh2$^{fl/fl}$ Mx-Cre B1-8i mice were injected with poly(I)•poly(C) and the B cell population was analyzed on day 10 after the last injection. At that time, deletion of *Ezh2* in the bone marrow was 100%. Expression of B1-8i heavy chain rescued B cell development in the bone marrow (**Fig. 4a**).

The low efficiency of the poly(I)•poly(C)-induced *Ezh2* inactivation in the peripheral B cells of Mx-Cre Ezh2$^{fl/fl}$ B1-8i mice (50%) precluded the possibility of analysis of B cell function in these mice. Nonetheless, high efficiency of poly(I)•poly(C)-induced Ezh2 inactivation in the bone marrow cells of Ezh2$^{fl/fl}$ Mx-Cre B1-8i mice allowed us to generate bone marrow chimeras carrying exclusively B1-8i–expressing Ezh2-deficient peripheral B cells. Transfer of bone marrow cells derived from poly(I)•poly(C)-injected Ezh2$^{fl/fl}$ Mx-Cre B1-8i mice into sublethally irradiated recombination-activating gene 1–deficient (RAG-1$^{-/-}$) mice resulted in the generation of subpopulations of developing bone marrow and peripheral B cells in the recipient mice that were similar to those observed in the donor mice (**Fig. 4b,c**). Ezh2-deficient peripheral B cells matured normally (**Fig. 4c**). Moreover, deficiency of Ezh2 did not affect Ig switch recombination *in vitro*, as shown by the wild-type frequencies of the

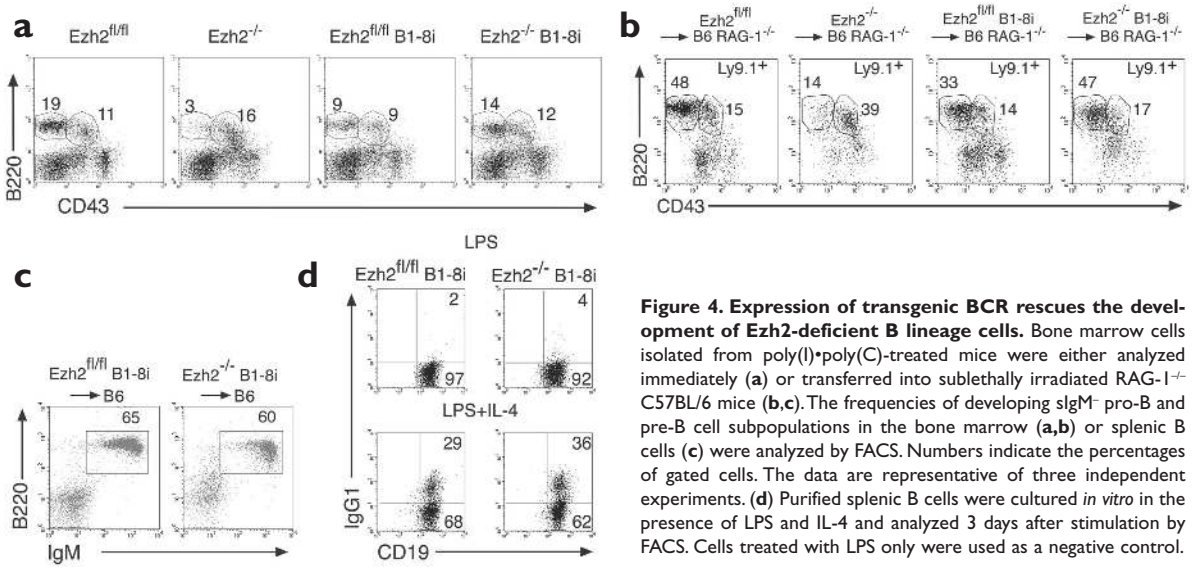

Figure 4. Expression of transgenic BCR rescues the development of Ezh2-deficient B lineage cells. Bone marrow cells isolated from poly(I)•poly(C)-treated mice were either analyzed immediately (**a**) or transferred into sublethally irradiated RAG-1$^{-/-}$ C57BL/6 mice (**b**,**c**). The frequencies of developing sIgM^{-} pro-B and pre-B cell subpopulations in the bone marrow (**a**,**b**) or splenic B cells (**c**) were analyzed by FACS. Numbers indicate the percentages of gated cells. The data are representative of three independent experiments. (**d**) Purified splenic B cells were cultured *in vitro* in the presence of LPS and IL-4 and analyzed 3 days after stimulation by FACS. Cells treated with LPS only were used as a negative control.

IgG1-positive cells induced by splenic B cell incubation with 10 μg/ml of LPS and 25 U/ml of interleukin 4 (IL-4) (**Fig. 4d**). This result suggests that lack of μ chain expression but not defective pre-BCR signaling is a chief cause of impaired B cell development in the absence of Ezh2.

Ezh2 is dispensable for peripheral B cells

Expression of the transgenic heavy chain may potentially mask changes in maturation and activation of peripheral Ezh2-deficient B cells. To achieve Ezh2 inactivation in peripheral B cells expressing a wild-type BCR repertoire, the Ezh2$^{fl/fl}$ mice were bred to mice expressing the Cre recombinase gene under control of the *Cd19* promoter (CD19-Cre)[30]. The analysis of Ezh2 mRNA expression in subpopulations of developing and peripheral B cells showed the presence of mRNAs corresponding to the wild-type and deleted *Ezh2* alleles in pro-B cells. Further B cell development was accompanied by loss of the wild-type Ezh2 mRNA expression (**Supplementary Fig. 4** online). Complete (100%) Ezh2 inactivation in peripheral B cells was also confirmed by Southern blot analysis (data not shown). The peripheral Ezh2-deficient B cells developed normally, as defined by membrane-bound expression of IgM and IgD (**Supplementary Fig. 4** online). Moreover *in vitro* proliferation of splenic B cells in response to anti–IgM F(ab)$_2$, anti-CD40 or LPS was not affected in the absence of Ezh2 (**Supplementary Fig. 4** online). Also Ezh2 deficiency had no impact on early BCR-mediated signaling, as defined by the wild-type–like kinetics of anti-IgM–induced calcium mobilization (**Supplementary Fig. 4** online). Thus, Ezh2 appears dispensable for the maturation and activation of peripheral B cells.

Ezh2 regulates V_HJ558 gene rearrangement

Next, we attempted to address the mechanism responsible for impaired μ chain expression in the absence of Ezh2. Reduced μ chain mRNA expression may result from inefficient V(D)J rearrangement, lower transcription of the rearranged *Igh* genes or decreased stability of the transcribed mRNA. The first possibility was addressed by the comparative analysis of *Igh* rearrangement in wild-type and Ezh2-deficient pro-B cells. The rearrangement of two different V_H gene families, V_H7183 and V_HJ558, was examined. The most fundamental difference between these families lies in their proximity to the DJ_H element. The V_H7183 family that consists of around 25 V_H genes is the smallest V_H gene family and is adjacent to the D_H segments at the most 3′ end of V_H gene locus[31]. Contrary to V_H7183, the V_HJ558 family is the largest and most frequently rearranged V_H gene family that occupies the most 5′ end to the middle of the V_H locus[31,32]. Two V_H gene primers, which are specific for most of the V_H gene segments within V_HJ558 family or V_H7183 family, respectively[33] were used to amplify the rearranged V_H to DJ_H1 or DJ_H2 sequences. The incidence of V_H to DJ_H joints involving V_H7183 segments was similar in control and Ezh2$^{-/-}$ pro-B cells (**Fig. 5a**). In contrast, recombination of V_HJ558 segments was reduced to 25% of the control (**Fig. 5a**). As a consequence, the amount of μ chain transcripts corresponding to V_HJ558 in pro-B cells was reduced to 11% of the wild-type, whereas μ chain transcripts expression corresponding to the V_H81X gene, the most prevalent gene within V_H7183 family, remained unaffected (**Fig. 5b**).

The discrepancy between 25% reduced V_HJ558 rearrangement and 11% reduced V_HJ558 mRNA levels could be explained by the presence of a substantial fraction of nonfunctional V_HJ558 rearrangements. Ig transcripts encoded by nonproductively rearranged $V_HD_HJ_H$ are unstable[34]. To test whether the reduction of μ chain V_HJ558 transcript in Ezh2-deficient pro-B cells reflected an increased frequency of nonfunctional $V_HD_HJ_H$ rearrangement, the individual $V_HD_HJ_H$ joints derived from the Ezh2$^{-/-}$ or control pro-B cells (B220$^+$CD43$^+$HSA$^+$BP-1$^+$) were amplified by PCR, sequenced and compared to the published V_H gene sequences. Productively rearranged $V_HD_HJ_H$ sequences were present in 60% of control and 20% of Ezh2$^{-/-}$ pro-B cells. In addition, the repertoire of V_HJ558 rearrangement was more diverse in control pro-B cells, whereas in Ezh2$^{-/-}$ pro-B cells, the V_H gene usage was restricted to a limited number of V_H gene segments (**Fig. 5c**). There was no major difference between control and Ezh2$^{-/-}$ pro-B cells in the percentage of productive V(D)J rearrangements and V_H gene usage within theV_H7183 family (**Fig. 5c**). This result shows the selective involvement of Ezh2 in V_HJ558 gene rearrangement.

Ezh2 does not control *Igh* germline transcription

Diminished rearrangement of V_HJ558 genes in Ezh2-deficient pro-B cells could be due to poor accessibility of this particular V_H locus to the recombination machinery. The degree of accessibility of the *Igh* locus correlates with transcription of the *Igh* genes in germline configuration (germline transcripts)[35]. The expression levels of different germline transcripts were analyzed in control and Ezh2$^{-/-}$ pro-B cells. The levels of germline transcripts of V_HJ558 were even higher in Ezh2$^{-/-}$ pro-B cells compared to control cells (**Fig. 6a**). The germline transcripts corresponding to proximal V_H genes such as V_H81X were equally abundant in control and Ezh2$^{-/-}$ pro-B cells. The expression levels of I_μ and μ_0 germline transcripts in control and

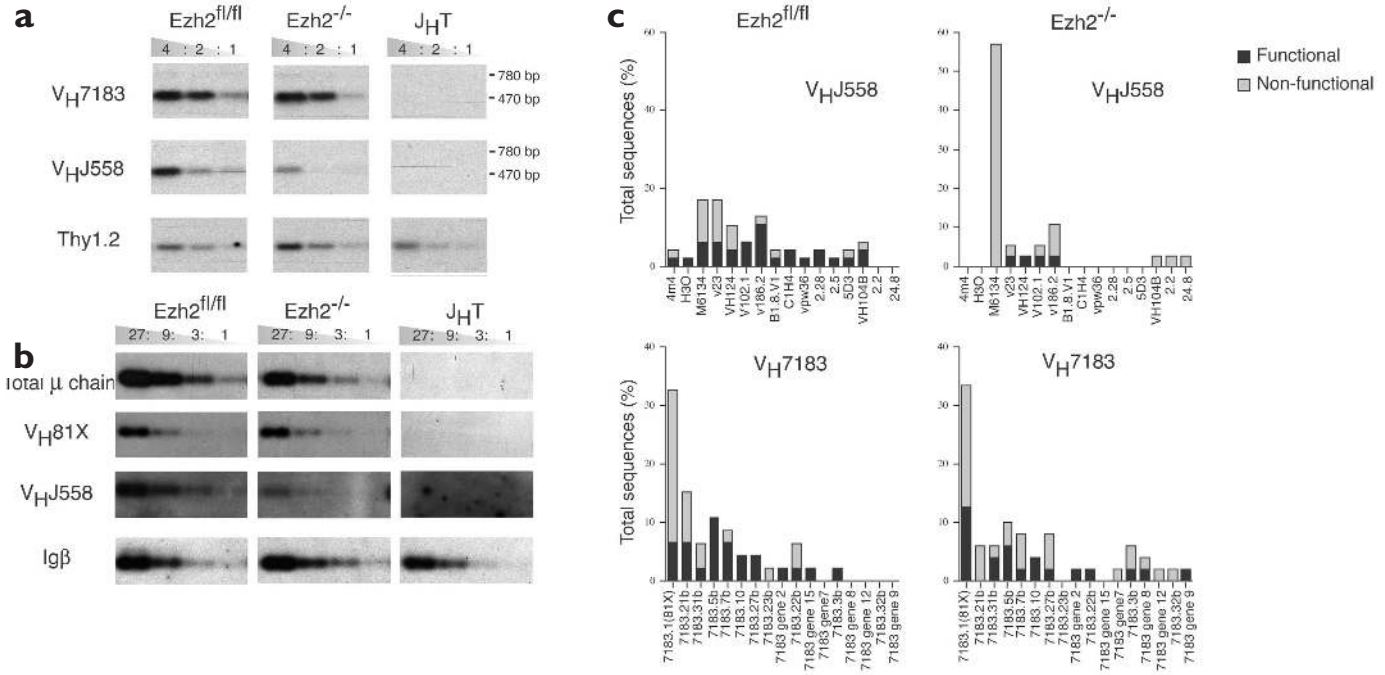

Figure 5. Impaired rearrangement and expression of V_HJ558 family genes in Ezh2-deficient pro-B cells. (**a**) Primers specific for V_H genes and primers recognizing the sequence 3′ downstream of J_H2 were used to amplify rearranged V_H to DJ_H1 (780-bp) and DJ_H2 (470-bp) from genomic DNA isolated from pro-B cells. DNA isolated from J_HT mice was used as a negative control. RT-PCR analysis of Thy1.2 mRNA expression was used as a cDNA loading control. (**b**) Degenerate primers that recognize most of the V_H genes (MsV_HE) and a μ constant region–specific primer (MsCμE) were used to amplify total μ chain transcript. μ chain transcripts corresponding to the V_H81X gene or V_HJ558 family were amplified with a specific set of primers (**Supplementary Table 1** online). The PCR products were visualized by Southern blotting with an IgH constant region–specific probe (MsCμN). RT-PCR analysis of Igβ mRNA expression was used as a cDNA loading control. (**c**) V_HJ558 and V_H7183 were amplified by PCR with DNA isolated from pro-B cells. The individual V_HD-$_HJ_H$ regions were sequence-analyzed with the DNAPLOT Program Package and Medline BLAST search. The V_H gene names or sequence accession numbers are indicated

$Ezh2^{-/-}$ pro-B cells were similar (**Fig. 6a**). The observed dichotomy between the levels of V_HJ558 genes germline transcription and V_HJ558 genes rearrangement suggest that another mechanism, unrelated to transcription, controls V_HJ558 gene rearrangement.

Ezh2-deficient cells are equipped for rearrangement

The expression levels of RAG-2, DNA-PK and Ku80 mRNAs, which are essential for the V(D)J recombination[36], were unaltered in Ezh2-deficient pro-B cells (**Supplementary Fig. 5** online). Furthermore, the analysis of the DNA double-stranded breaks (DSBs) that occur during the course of V_HJ558 to DJ_H rearrangement[35] did not reveal an accumulation of the signal and coding ends in Ezh2-deficient pro-B cells (**Supplementary Fig. 5** online). These results suggest that Ezh2-deficient pro-B cells are well equipped for V(D)J rearrangement, and those recombination events that are initiated should be completed.

Ezh2-deficient pro-B cells live and divide normally

In B cell ontogeny, the proximal V_H7183 genes are preferentially rearranged in the pro-B cells[32], whereas B cells possessing V_HJ558 heavy chains expand at later stages of B cell development[37]. If Ezh2 controls

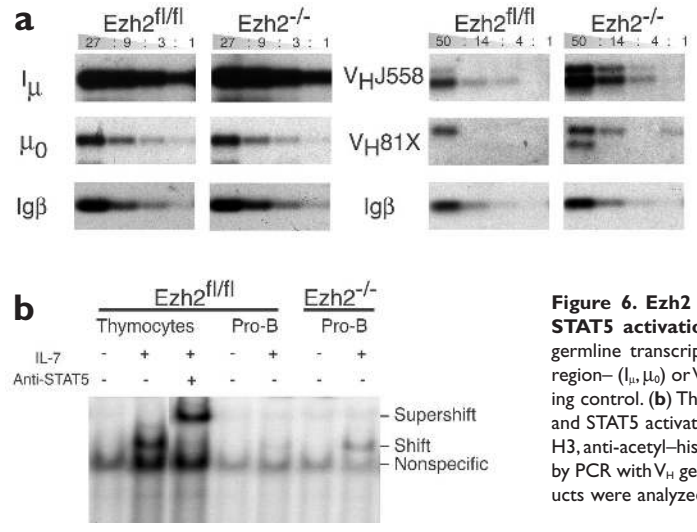

Figure 6. Ezh2 does not control expression of IgH germline transcripts, IL-7–mediated STAT5 activation or histone acetylation in pro-B cells. (**a**) Expression levels of $I_μ$, $μ_0$ and V_H germline transcripts in pro-B cells were analyzed by RT-PCR and Southern blotting with μ constant region– ($I_μ$, $μ_0$) or V_H–specific probes. RT-PCR analysis of Igβ mRNA expression was used as a cDNA loading control. (**b**) Thymocytes or pro-B cells were incubated in the presence or absence of IL-7 (20 ng/ml) and STAT5 activation was analyzed by EMSA. (**c**) ChIP was done on pro-B cells with anti-acetyl–histone H3, anti-acetyl–histone H4 or without antibody (negative control). The coprecipitated DNA was analyzed by PCR with V_H gene–specific primers or primers recognizing the $E_μ$ enhancer region, then the PCR products were analyzed by Southern blotting with specific probes.

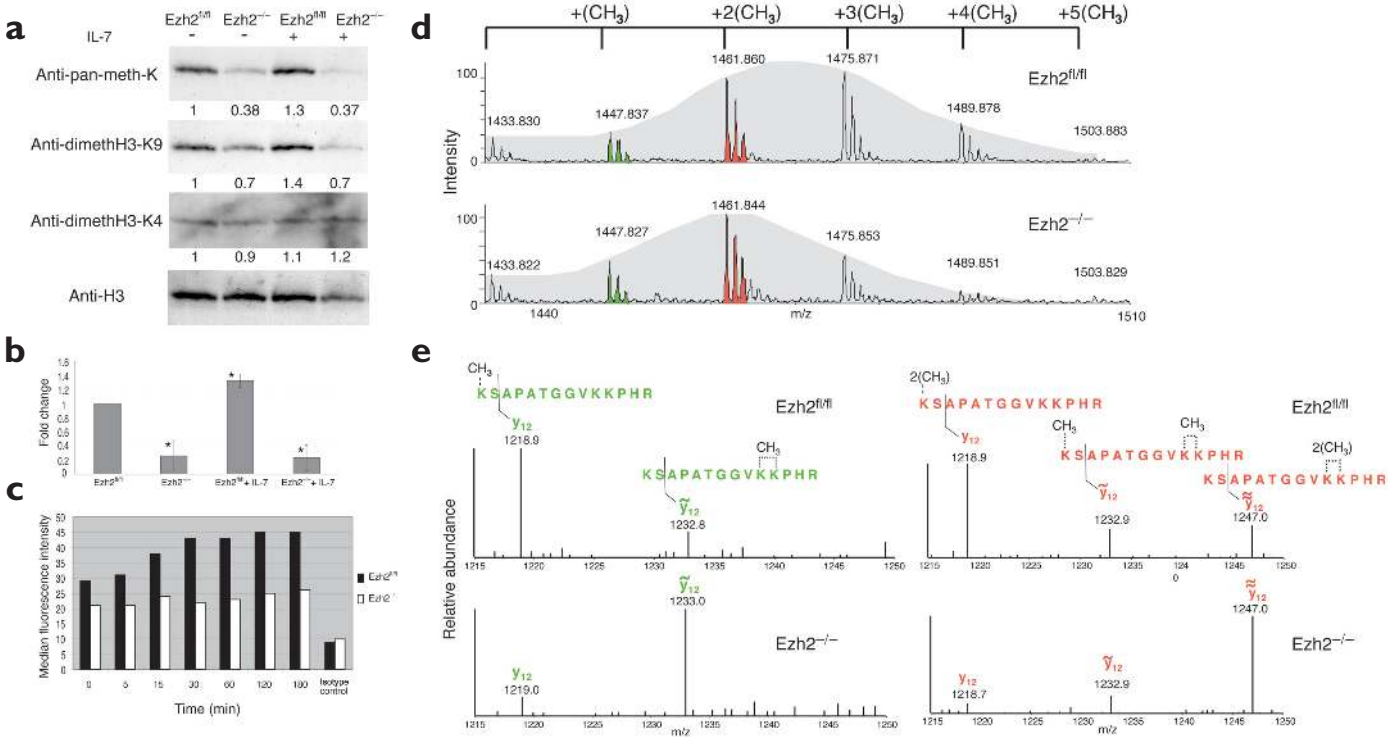

Figure 7. Reduced lysine methylation of histone H3 in Ezh2-deficient pro-B cells. Methylation of histone H3 in nuclear lysates of pro-B cells incubated with or without IL-7 was analyzed by immunoblotting with anti-pan–methyl-lysine (**a,b**), anti-dimethyl–histone H3-K9 or anti-dimethyl– histone H3-K4 (**a**). The amount of histone H3 loading was controlled for by immunoblotting with anti–histone H3. The numbers indicate fold changes compared to the signal of the unstimulated control lysate once it had been normalized against the amount of histone H3 (**a**). Fold changes from four independent experiments are summarized in b. Bars represent mean ± s.d. data. The differences between control pro-B cells that didn't or did receive IL-7 stimulation were statistically significant and are indicated by asterisks (Student's *t*-test, $P < 0.005$). (**c**) Kinetics of IL-7–induced methylation. The levels of intracellular lysine methylation were analyzed by FACS. The median fluorescence intensity of methylated lysine staining at each time point is shown. (**d**) Portion of the mass spectra of tryptic digests of histone H3 comparing methylation of the peptide 27KSAPATGGVKKPHR40 from pro-B cells. The degree of methylation of the peptide is indicated and the different extents of methylation are accentuated by the shaded envelopes. The singly and doubly methylated peptide ions with *m/z* 1447.8 and 1461.8 were further studied by MS-MS. (**e**) Portion of the MS-MS spectrum of the *m/z* 1447.8 singly methylated ion (left panel) and *m/z* 1461.8 doubly methylated ion (right panel) showing the change in methylation of K27 to K36, K37. The change in methylation is reflected by the change in intensities of the y_{12}-type fragments. The MS-MS spectrum of the singly methylated ion (left panel) reveals the presence of two ion species with the same mass but having different sites of methylation, whereas the doubly methylated ion (right panel) reveals the presence of three ion species with the same mass but with different sites of methylation. Changes in methylation can be followed by changes in the ratios of these fragmentation ion intensities. (**f**) Chromatin immunoprecipitation was done on pro-B cells with anti-pan–methyl-lysine. The coprecipitated DNA was analyzed by PCR with primers specific for the V_HJ558 and V_H81X genes. The PCR products were analyzed by Southern blotting with internal probes.

pro-B cell survival, the observed changes in V_HJ558 rearrangement may simply reflect the premature death of Ezh2-deficient pro-B cells prior to completion of V_HJ558 rearrangement. However the viability of pro-B cells, as defined by terminal deoxynucleotidyltransferase–mediated dUTP-biotin nick end–labeling (TUNEL) assay or intracellular staining of activated caspases, was not affected by Ezh2 deficiency (**Supplementary Fig. 6** online).

The regulation of V(D)J recombination is coupled to the cell cycle[38]. The RAG-1 and RAG-2 proteins are abundant during the G1 phase and V(D)J recombination is prohibited during S and M phase[38]. Hence changes in the cell cycle progression could possibly affect the Igh rearrangement. However, unaltered cell cycle parameters of Ezh2-deficient pro-B cells shown by *in vivo* 5-bromodeoxyuridine (BrdU) labeling argued against such possibility. (**Supplementary Fig. 6** online). Thus, the *Igh* rearrangement defect in Ezh2-deficient pro-B cells was not due to poor survival of the cells or defective cell cycle progression.

Unimpaired STAT5 activation and histone acetylation

Igh rearrangement in general and histone acetylation of the V_HJ558 locus is regulated by IL-7[39,40]. However, IL-7Rα expression and the IL-7–induced activation of STAT5[41] were not reduced in Ezh2$^{-/-}$ CD19$^+$IgM$^-$ B cell progenitors (**Fig. 6b** and **Supplementary Fig. 7** online). Moreover, the acetylation of histones H3 and H4 associated with *Igh* locus was not impaired by Ezh2 deficiency (**Fig. 6c**). This result shows that Ezh2 does not control IL-7 signaling upstream of STAT5 or signaling that leads to histone H3 and H4 acetylation.

Ezh2 methylates histone H3 in pro-B cells

The SET domain of Ezh2 may possess HMTase activity similar to E(Z), which could result in impaired histone H3 methylation in Ezh2-deficient cells. Immunoblot analysis of histone H3 methylation with pan–methyl-lysine–specific antibody revealed reduced histone H3 lysine methylation in the Ezh2-deficient pro-B cells (62% reduction), compared to control pro-B cells (**Fig. 7a**). Incubation of control pro-B cells with IL-7 (20 ng/ml) caused a modest but consistent increase of lysine methylation, as determined by immunoblotting and fluorescence-activated cell sorting (FACS) (**Fig. 7a–c** and **Supplementary Fig. 8** online). In contrast, incubation of Ezh2-deficient cells with IL-7 did not increase histone H3 lysine methylation (**Fig. 7a–c**). Methylation was unaltered at H3 lysine at position 4 (H3-K4) and a modest reduction of H3 lysine 9 (H3-K9)

methylation suggested that another lysine residue is controlled by Ezh2 *in vivo*. To reveal the lysine residue within H3 that might be responsible for the observed changes in H3 methylation, we employed mass- and tandem-mass spectrometry (MS-MS) analysis[42,43] of methylation in histone H3 (**Fig. 7d,e**). The mass spectra of the proteolytic mixtures obtained by trypsin digestion of histone H3 derived from the wild-type and Ezh2-deficient pro-B cells were analyzed. MS-MS analysis showed that this methylation change occurred primarily at K27, where methylation was attenuated by more than five-fold in Ezh2-deficient pro-B cells compared to controls (**Fig. 7e**). Although observed changes in histone methylation appeared to be global, they affected the methylation status of histones associated with V_HJ558 or V_H7183 genes differently (**Fig. 7f**). In the wild-type pro-B cells, the histone associated with the V_H81X locus (V_H7183 family) was hypomethylated compared to methylated histone linked to the V_HJ558 locus (**Fig. 7f**). As a consequence, Ezh2 deficiency has a clear effect on methylation of the V_HJ558 but not V_H81X locus–associated histone. These data explain the selective impact of Ezh2 deficiency on V_HJ558 gene rearrangement.

Discussion

Ezh2 deficiency leads to diminished generation of pre-B cells and immature B cells in the bone marrow. Defective B cell development cannot be restored by the presence of the wild-type cells in the mixed bone marrow chimeras, thus supporting the B lineage–autonomous nature of the observed defect. The unaltered *in vivo* maturation and *in vitro* activation of B cells that acquire Ezh2 deficiency at post–pro-B cell stages show that the requirement for Ezh2 is development stage–specific. It could well be that Ezh1, which is abundant mostly in mature B cells, compensates for loss of Ezh2.

The cause of impaired Ezh2-deficient B cell development lies in reduced rearrangement of the V_HJ558 gene cluster. The fact that the V_HJ558 family of V_H genes comprises the largest V_H gene family in mouse genome[31] explains the reduction in the number of intracellular μ chain–positive Ezh2-deficient pro-B cells.

The absence of Ezh2 reduces both the basal and IL-7–induced histone H3 lysine methylation. This reduction is mainly due to the diminished methylation at lysine 27 (H3-K27). Our results show that similar to the *Drosophila* protein E(Z)[15–17], murine Ezh2 is an HMTase with H3-K27 specificity. Furthermore, we have also demonstrated the ability of an extracellular ligand, IL-7, to control chromatin structure *via* inducible histone H3 methylation. Because histone methylation is considered to be irreversible[44], even the modest increase in methylation observed in IL-7–stimulated pro-B cells is likely to have a long-lasting impact on the chromatin structure.

The mechanism of histone H3 methylation induction by IL-7 remains elusive. The wild-type–like activation of signal transducers and activators of transcription 5 (STAT5), a key signaling component downstream of the IL-7R[41], makes an involvement of STAT5 in IL-7 induced methylation unlikely. Moreover, unaltered H3 acetylation excludes a possible indirect effect of Ezh2-deficiency on H3 methylation through changes in histone acetylation. Overall, these data suggest the existence of STAT5-independent signaling connecting IL-7R and histone H3 methylation through Ezh2.

Given the critical role played by IL-7 in the regulation of V(D)J rearrangement[41], in particular of V_HJ558 genes[39,40], it is plausible that Ezh2-dependent histone H3 methylation provides the mechanism by which IL-7 targets the recombination machinery to the *Igh* locus. Despite the seemingly global role of Ezh2 in histone H3 methylation, methylated histone associated with V_HJ558 or V_H7183 genes is not equally affected by Ezh2 deficiency. Hence, within the *Igh* locus, Ezh2 seems to play a selective role in the regulation of V_HJ558 methylation and recombination. Because neither histone acetylation nor V_H gene germline transcription are affected by Ezh2 deficiency, a mechanism other than transcription must be important for V(D)J rearrangement.

The histone code hypothesis[45] postulates that covalent modification of histones, including acetylation and methylation, promotes binding of specific proteins to chromatin to alter transcription[45], the DNA double-strand break (DSB) repair[46] and DNA excision[47]. The lack of accumulation of unrepaired DSBs within the V_HJ558 locus in Ezh2-deficient pro-B cells suggests that DNA cleavage rather than repair are affected by the absence of Ezh2. Therefore, we speculate that Ezh2-mediated histone H3 methylation may facilitate targeting of recombination machinery, including RAG proteins, which catalyzes the DNA cleavage or is responsible for marking the borders of the DNA excision, similar to the histone methylation–dependent mechanism responsible for programmed DNA elimination that accompanies macronuclear development in *Tetrahymena*[47]. Overall, we have identified novel mechanism of regulation of B cell development through Ezh2-mediated histone H3 methylation. In view of the role of Ezh2 in *Igh* rearrangement, it remains to be seen whether related processes such as Ig switch recombination and somatic hypermutation are regulated by histone methylation.

Methods

Generation of mice with a *loxP*-flanked *Ezh2* allele. A 3.5-kb *Kpn*I fragment of *Ezh2* (**Fig. 2**) was inserted into the *Cla*I site of pKSTKNEOLOXP between the *loxP*-flanked *neo*^{r} expression cassette (*neo*^{r}) and gene encoding TK. A 3.5-kb *Kpn*I-*Bam*HI fragment containing the exons encoding SET domain was inserted into the *Sal*I site between *neo*^{r} and the *loxP* site. Finally, a 3.5-kb *Bam*HI-*Mam*I fragment was cloned into the *Not*I site located 3′ of the *loxP* site. The *Sac*II-linearized DNA of the Ezh2 targeting vector (pKSTKNEOLOXP-Ezh2-SET#15) was transfected by electroporation into E14-1.1 cells[48] followed by their selection in the presence of G418 (300 μg/ml) and gancyclovir (2 μM). The DNA of double-resistant ES cells was digested with *Bam*HI and tested for homologous recombination by Southern blot analysis with a 1-kb *Mam*I-*Eco*RI DNA fragment as a probe (probe A). This probe recognizes 19-kb and 24.5-kb DNA fragments corresponding to the wild-type and targeted loci, respectively. To delete the *loxP*-flanked *neo*^{r} gene, the ES cell clones carrying the targeted *Ezh2* allele were transiently transfected with 10 μg of the Cre-recombinase expression vector pIC-Cre[22]. DNA from neomycin-sensitive clones was analyzed for *neo*^{r} deletion by Southern blot analysis with probe A and selected ES clones were injected into blastocysts to generate chimeras and later mice carrying *loxP*-modified *Ezh2*. Heterozygous Ezh2$^{fl/+}$ mice were bred to Mx-Cre mice[26] to generate Ezh2$^{fl/+}$ Mx-Cre mice that were crossed to generate Ezh2$^{fl/fl}$ Mx-Cre$^{+/-}$ mice. Mice were genotyped for the presence of the *loxP*-floxed *Ezh2* allele and Mx-Cre transgene by Southern blotting and PCR. The primers used are listed in **Supplementary Table 1** online. The efficiency of inducible Mx-Cre–mediated Ezh2 deletion was determined by Southern blot analysis of the *Eco*RI-digested genomic DNA isolated from various lymphoid organs. The results were quantified with the NIH Image 1.62 program. All mice were bred and maintained under specific pathogen–free conditions at the Laboratory Animal Research Center of the Rockefeller University; all mouse protocols were approved by the Rockefeller University IACUC.

FACS analysis and cell sorting. The preparation of *ex vivo*–isolated cells for FACScan analysis and sorting of the lymphocyte subpopulations on FACSstar was done as described[49]. The analysis of the BrdU-labeled cells and TUNEL assay were performed with a BrdU flow kit (BD Pharmingen, San Diego, CA) and a Fluorescein In Situ Cell Death Detection Kit (Roche, Indianapolis, IN) according to the manufacturer's protocol. Analysis of activated caspases was performed with a CaspaTag Fluorescein Caspase (VAD) Activity Kit (Intergen, Norcross, GA) according to the manufacturers' protocol. The antibodies anti-B220 (RA3-6B2), anti-CD43 (S7), anti-IgD (11-26c.2a), anti-Ly51 (BP-1), anti-IgG1 (RB6-8C5), anti-HSA (M1/69), anti-CD127 and anti-Ly9.1 were purchased from BD Pharmingen. Anti-IgM was purchased from Jackson ImmunoResearch (West Grove, PA). Phycoerythrin (PE)-Cy7 and cychrome-streptavidin were obtained from Caltag. Anti–IL-7Rα (R7A34), anti–μ chain (M41) and anti–κ chain (R33-18-10) were prepared from the corresponding hybridoma (a gift of K. Rajewsky). For MACS, cells were incubated with the appropriate magnetic beads (Miltenyi Biotec, Auburn, CA) and purified as described[49]. The purity of isolated population was controlled by FACS analysis. Purified cells for further experiments were at least 95% pure.

RNA isolation, cDNA synthesis and PCR. Total RNA was isolated from 1×10^5 purified lymphocyte subpopulations with TRIzol reagent (Gibco-BRL, Gaithersburg, MD) and cDNA was synthesized with the First Strand cDNA Synthesis Kit (Gibco-BRL). PCR reactions were performed on a pelitier thermal cycler (PTC 200, MJ Research, Waltham, MA). The primer sequences used in the experiments and references are listed in **Supplementary Table 1** online.

EMSA. Cells were washed once with PBS after stimulation and resuspended in lysis buffer (20 mM HEPES at pH 7.5, 450 mM NaCl, 0.4 mM EDTA, 0.5 mM dithiothreitol, 25% glycerol, 0.5 mM 4-(2-aminoethyl)-benzenesulfonyl fluoride hydrochloride (AEBSF), 10 mM NaF, 1 μg/ml of leupeptin, 2 μg/ml of aprotinin and 5 mM Na_3VO_4). Samples were subjected to three freeze-thaw cycles. Whole cell extracts were prepared by spinning at 10,000*g* at 4 °C for 15 min. Extracts (20 μg) in 10 μl of lysis buffer were combined with 11 μl of 2X binding buffer (100 mM KCl, 20 mM Tris-HCl, 20 mM HEPES, 1 mM dithiothreitol, 1 mM EDTA and 20% glycerol) containing 1 μg of poly (dI)·(dC) (Amersham, Piscataway, NJ) and incubated for 20 min on ice. For the supershift, 1 μl (0.2 μg) of STAT5b antiserum (Santa Cruz Biotechnology, Santa Cruz, CA) was added to the samples. After a 20-min incubation, 0.4 ng of a radioactive [γ^{32}P]dATP-labeled probe, derived from ovine β-casein (Santa Cruz Biotechnology), was added and incubated for further 20 min on ice. Samples were resolved on the 5% polyacrylamide native gels and analyzed after dry gel exposure to x-ray film at –80 °C.

ChIP. Purified pro-B cells (1×10^6) were washed once with PBS and fixed by adding formaldehyde to a final concentration 0.37% for 10 min at 37 °C. ChIP assays were performed with the Chromatin Immunoprecipitation Assay Kit (Upstate Biotechnology, Grand Island, NY) according to manufacturer's protocol. Anti-acetyl–histone H3 and H4 (Upstate Biotechnology) and anti-pan–methyl-lysine (Abcom, Cambridge, UK) were used for immunoprecipitation. The primers used in the experiments have been described[40]. The oligoprobes used for the Southern blot analysis are listed in **Supplementary Table 1** online.

LM-PCR. DNA from 2×10^5 sorted pro-B cells was isolated with the agarose plug method. The agarose DNA plugs were subjected to linker ligation for 18 h at 16 °C in 12 μl of ligation buffer (Boehringer Mannheim, Mannheim, Germany) with 48 pmol of linker and 3U of T4 ligase; 1 μl of DNA was used for each PCR reaction. The PCR products were resolved on 1.5% agarose gel and transferred to nitrocellulose membrane. The specific bands were visualized by hybridization with a radioactive labeled internal probe.

Immunoblot analysis. Immunoblot analysis was performed with standard procedures[50] with the use of nuclear lysate. The nuclei were isolated by incubating cell with nuclei-extraction buffer (320 mM sucrose, 5 mM $MgCl_2$, 10 mM HEPES and 1% Triton X-100 at pH 7.4) on ice for 10 min, followed by double washing with wash buffer (320 mM sucrose, 5 mM $MgCl_2$ and 10 mM HEPES). The nuclei were resuspended in sonication buffer (50 mM Tris at pH 8, 500 mM NaCl, 1 mM EDTA and 10% glycerol) and subjected to sonication to break the nuclear membrane and extract the nuclear protein. Purified anti–mouse Ezh2 rabbit serum (provided by T. Jenuwein, IMP, Austria), rabbit anti-pan–methyl-lysine (Abcam), rabbit anti-dimethyl–histone H3 lysine 9, rabbit anti-dimethyl–histone H3 lysine 4 (Upstate Biotechnology) and goat anti–histone H3 (N-20) (Santa Cruz Biotechnology) were used in the immunoblotting. Horseradish peroxidase (HRP)–anti-rabbit (Amersham) and HRP–anti-goat (Sigma, St. Louis, MO) were used as secondary antibodies. The signal was detected by the chemiluminescence system (Supersignal, Pierce, Rockford, IL) and quantified with the NIH Image 1.62 program.

Mass spectrometry analysis. Mass spectra of the proteolytic mixtures obtained by trypsin digestion of histone H3 were obtained with an in-house–modified MALDI-QqTOF mass spectrometer[43] with a compact disc (CD) sample stage[42]. Masses of the tryptic fragments were determined with an accuracy of 10 ppm. After obtaining the tryptic peptide mass map, the CD sample stage was transferred to an in-house–constructed MALDI-ion trap mass spectrometer for detailed MS-MS analysis of the tryptic peptide ions[42].

Web addresses. The DNAPLOT Program Package can be located at http://www.dnaplot.org.

Note: Supplementary information is available on the Nature Immunology *website*.

Competing interests statement

The authors declare that they have no competing financial interests.

Acknowledgments

We thank M. Nussenzweig, K. Rajewsky, C. Schmedt, K. Saijo, I. Mecklenbräuker and D. O'Carroll for discussions. We also thank G. Hannon for critical review of this manuscript. Supported by The Irene Diamond Fund (A.T.), National Institutes of Health grant (A.T.), NIH, RR0086 (B.T.C.) and The Rockefeller University's Norman and Rosita Winston Fellowship Program (I.S.).

Received 9 October 2002; accepted 22 November 2002.

1. Francis, N.J. & Kingston, R.E. Mechanisms of transcriptional memory. *Nat Rev. Mol. Cell Biol.* **2**, 409–421 (2001).
2. Mahmoudi, T. & Verrijzer, C.P. Chromatin silencing and activation by Polycomb and trithorax group proteins. *Oncogene* **20**, 3055–3066 (2001).
3. Franke, A. *et al.* Polycomb and polyhomeotic are constituents of a multimeric protein complex in chromatin of Drosophila melanogaster. *EMBO J.* **11**, 2941–2950 (1992).
4. van Lohuizen, M. *et al.* Interaction of mouse polycomb-group (Pc-G) proteins Enx1 and Enx2 with Eed: indication for separate Pc-G complexes. *Mol. Cell. Biol.* **18**, 3572–3579 (1998).
5. Sewalt, R.G. *et al.* Characterization of interactions between the mammalian polycomb-group proteins Enx1/Ezh2 and EED suggests the existence of different mammalian polycomb-group protein complexes. *Mol. Cell. Biol.* **18**, 3586–3595 (1998).
6. Shao, Z. *et al.* Stabilization of chromatin structure by PRC1, a Polycomb complex. *Cell* **98**, 37–46 (1999).
7. Gould, A. Functions of mammalian Polycomb group and trithorax group related genes. *Curr. Opin. Genet. Dev.* **7**, 488–494 (1997).
8. van der Lugt, N.M. *et al.* Posterior transformation, neurological abnormalities, and severe hematopoietic defects in mice with a targeted deletion of the bmi-1 proto-oncogene. *Genes Dev.* **8**, 757–769 (1994).
9. Katoh-Fukui, Y. *et al.* Male-to-female sex reversal in M33 mutant mice. *Nature* **393**, 688–692 (1998).
10. Akasaka, T. *et al.* The role of mel-18, a mammalian Polycomb group gene, during IL-7-dependent proliferation of lymphocyte precursors. *Immunity* **7**, 135–146 (1997).
11. Tokimasa, S. *et al.* Lack of the Polycomb-group gene rae28 causes maturation arrest at the early B-cell developmental stage. *Exp. Hematol.* **29**, 93–103 (2001).
12. Core, N. *et al.* Altered cellular proliferation and mesoderm patterning in Polycomb-M33-deficient mice. *Development* **124**, 721–729 (1997).
13. Hobert, O., Jallal, B. & Ullrich, A. Interaction of Vav with ENX-1, a putative transcriptional regulator of homeobox gene expression. *Mol. Cell. Biol.* **16**, 3066–3073 (1996).
14. Hobert, O., Sures, I., Ciossek, T., Fuchs, M. & Ullrich, A. Isolation and developmental expression analysis of Enx-1, a novel mouse Polycomb group gene. *Mech. Dev.* **55**, 171–184 (1996).
15. Czermin, B. *et al.* Drosophila enhancer of zeste/ESC complexes have a histone H3 methyltransferase activity that marks chromosomal polycomb Sites. *Cell* **111**, 185–196 (2002).
16. Muller, J. *et al.* Histone methyltransferase activity of a Drosophila polycomb group repressor complex. *Cell* **111**, 197–208 (2002).
17. Cao, R. *et al.* Role of histone H3 lysine 27 methylation in Polycomb-group silencing. *Science* **298**, 1039–1043 (2002).
18. Kouzarides, T. Histone methylation in transcriptional control. *Curr. Opin. Genet. Dev.* **12**, 198–209 (2002).
19. Raaphorst, F.M. *et al.* Coexpression of BMI-1 and Ezh2 polycomb group genes in Reed-Sternberg cells of Hodgkin's disease. *Am. J. Pathol.* **157**, 709–715 (2000).
20. Fukuyama, T. *et al.* Proliferative involvement of ENX-1, a putative human polycomb group gene, in haematopoietic cells. *Br. J. Haematol.* **108**, 842–847 (2000).
21. O'Carroll, D. *et al.* The polycomb-group gene Ezh2 is required for early mouse development. *Mol. Cell. Biol.* **21**, 4330–4336 (2001).
22. Gu, H., Zou, Y.R. & Rajewsky, K. Independent control of immunoglobulin switch recombination at individual switch regions evidenced through Cre-loxP-mediated gene targeting. *Cell* **73**, 1155–1164 (1993).
23. Laible, G. *et al.* Mammalian homologues of the Polycomb-group gene Enhancer of zeste mediate gene silencing in Drosophila heterochromatin and at S. cerevisiae telomeres. *EMBO J.* **16**, 3219–3232 (1997).
24. Tschiersch, B. *et al.* The protein encoded by the Drosophila position-effect variegation suppressor gene Su(var)3-9 combines domains of antagonistic regulators of homeotic gene complexes. *EMBO J.* **13**, 3822–3831 (1994).
25. Carrington, E.A. & Jones, R.S. The Drosophila Enhancer of zeste gene encodes a chromosomal protein: examination of wild-type and mutant protein distribution. *Development* **122**, 4073–4083 (1996).
26. Kühn, R., Schwenk, F., Aguet, M. & Rajewsky, K. Inducible gene targeting in mice. *Science* **269**, 1427–1429 (1995).
27. Baird, A.M., Gerstein, R.M. & Berg, L.J. The role of cytokine receptor signaling in lymphocyte development. *Curr. Opin. Immunol.* **11**, 157–166 (1999).
28. Kitamura, D., Roes, J., Kühn, R. & Rajewsky, K. A B cell-deficient mouse by targeted disruption of the membrane exon of the immunoglobulin mu chain gene. *Nature* **350**, 423–426 (1991).
29. Sonoda, E. *et al.* B cell development under the condition of allelic inclusion. *Immunity* **6**, 225–233 (1997).
30. Rickert, R.C., Roes, J. & Rajewsky, K. B lymphocyte-specific, Cre-mediated mutagenesis in mice. *Nucleic Acids Res.* **25**, 1317–1318 (1997).
31. Wu, G.E. & Paige, C.J. VH gene family utilization in colonies derived from B and pre-B cells detected by the RNA colony blot assay. *EMBO J.* **5**, 3475–3481 (1986).
32. Connor, A.M. *et al.* Mouse VH7183 recombination signal sequences mediate recombination more frequently than those of VHJ558. *J. Immunol.* **155**, 5268–5272 (1995).
33. Ehlich, A. *et al.* Immunoglobulin heavy and light chain genes rearrange independently at early stages of B cell development. *Cell* **72**, 695–704 (1993).
34. Li, S. & Wilkinson, M.F. Nonsense surveillance in lymphocytes? *Immunity* **8**, 135–141 (1998).
35. Schlissel, M.S. & Stanhope-Baker, P. Accessibility and the developmental regulation of V(D)J recombination. *Semin. Immunol.* **9**, 161–170 (1997).
36. Grawunder, U. & Harfst, E. How to make ends meet in V(D)J recombination. *Curr. Opin. Immunol.* **13**, 186–194 (2001).
37. Malynn, B.A., Yancopoulos, G.D., Barth, J.E., Bona, C.A. & Alt, F.W. Biased expression of JH-proximal VH genes occurs in the newly generated repertoire of neonatal and adult mice. *J. Exp. Med.* **171**, 843–859 (1990).
38. Lin, W.C. & Desiderio, S.V(D)J recombination and the cell cycle. *Immunol. Today* **16**, 279–289 (1995).
39. Corcoran, A.E., Riddell, A., Krooshoop, D. & Venkitaraman, A.R. Impaired immunoglobulin gene rearrangement in mice lacking the IL-7 receptor. *Nature* **391**, 904–907 (1998).
40. Chowdhury, D. & Sen, R. Stepwise activation of the immunoglobulin mu heavy chain gene locus. *EMBO J.* **20**, 6394–6403 (2001).
41. Hofmeister, R. *et al.* Interleukin-7: physiological roles and mechanisms of action. *Cytokine Growth Factor Rev.* **10**, 41–60 (1999).
42. Krutchinsky, A.N., Kalkum, M. & Chait, B.T. Automatic identification of proteins with a MALDI-quadrupole ion trap mass spectrometer. *Anal. Chem.* **73**, 5066–5077 (2001).
43. Krutchinsky, A.N., Zhang, W. & Chait, B.T. Rapidly switchable matrix-assisted laser desorption/ionization and electrospray quadrupole-time-of-flight mass spectrometry for protein identification. *J. Am. Soc. Mass Spectrom.* **11**, 493–504 (2000).
44. Bannister, A.J., Schneider, R. & Kouzarides, T. Histone methylation: dynamic or static? *Cell* **109**, 801–806 (2002).
45. Strahl, B.D. & Allis, C.D. The language of covalent histone modifications. *Nature* **403**, 41–45 (2000).
46. Bird, A.W. *et al.* Acetylation of histone H4 by Esa1 is required for DNA double-strand break repair. *Nature* **419**, 411–415 (2002).
47. Taverna, S.D., Coyne, R.S. & Allis, C.D. Methylation of histone H3 at lysine 9 targets programmed DNA elimination in tetrahymena. *Cell* **110**, 701–711 (2002).
48. Torres, R.M. & Kühn, R. Cre/loxP recombination system and gene targeting. *Meth. Mol. Biol.* **180**, 175–204 (2002).
49. Mecklenbräuker, I., Saijo, K., Zheng, N.Y., Leitges, M. & Tarakhovsky, A. Protein kinase Cδ controls self-antigen-induced B-cell tolerance. *Nature* **416**, 860–865 (2002).
50. Sambrook, J., Fritsch, E.F. & Maniatis, T. *Molecular Cloning* (Cold Spring Harbor Laboratory Press, New York, 1989).